NJC

Nickel oxide nanoparticles/ionic liquid crystal modified carbon composite electrode for determination of neurotransmitters and paracetamol

Journal:	*New Journal of Chemistry*
Manuscript ID	NJ-ART-07-2015-001804.R1
Article Type:	Paper
Date Submitted by the Author:	16-Oct-2015

Complete List of Authors:	Atta, Nada; Faculty of Science, University of Cairo, Egypt, Department of Chemistry Ibrahim, Asmaa; Organization for Drug Control and Research , Pharmaceutical Chemistry Galal, Ahmed; Cairo University, Faculty of Science, Chemistry

Nickel oxide nanoparticles/ionic liquid crystal modified carbon composite electrode for determination of neurotransmitters and paracetamol

Nada F. Atta*, Asmaa H. Ibrahim, Ahmed Galal
[1]Chemistry Department, Faculty of Science, Cairo University, 12013 Giza, Egypt
Tel.: +20 0237825266; fax: +20 0235727556, anada@sci.cu.edu.eg

Abstract

Ionic liquid crystal 1-butyl-1-methyl-piperidinium hexa-fluoro-phosphate and nickel oxide nanoparticles were used to construct a carbon composite electrode. This novel composite was used successfully as a sensor platform for the determination of paracetamol and some neurotransmitters such as dopamine, norepinephrine, levodopa and serotonin. Several advantages are realized in this approach, the unique properties of nanomaterials and ionic liquid crystals, and the ease of fabrication of the carbon composite electrode. The modified sensor was evaluated and compared with nickel oxide nanoparticles/ionic liquid modified electrodes in presence of surfactant, namely 1-n-hexyl-3-methyl imidazolium tetra-fluoro-borate and 1-butyl-4-methyl pyridinium tetra-fluoro-borate for the electrocatalytic oxidation of paracetamol. Modification with ionic liquid crystals showed superior current signals compared to ionic liquids. The interaction of surfactants with neurotransmitters resulted in preconcentration of the drug at the ionic liquid crystal interface that allowed both ionic channeling and charge transfer mediation. Figures of merits with optimized performance are: a linear dynamic range of 44.4×10^{-7} - 2.78×10^{-4} mol L^{-1} for paracetamol sensing with a correlation coefficient 0.999 and limit of detection of 8.61×10^{-9} mol L^{-1}. The electrode was successfully employed for direct determination of paracetamol in human urine samples, for its assay in pharmaceutical formulations and its simultaneous determination in presence of neurotransmitters. High reproducibility and selectivity in presence of potential interfering species were ascertained for this electrode.

Keywords: Ionic liquid crystals; Nickel oxide nanoparticles; Surfactants; Acetaminophen; Neurotransmitters; Carbon composite electrode.

1. Introduction:

Acetaminophen (N-acetyl-p-aminophenol or Paracetamol) (ACOP) is one of the most common drugs used in the world and has a similar structure to aspirin. Acetaminophen

acts as a pain-killer by inhibiting prostaglandin's synthesis in the central nervous system and relieves fever. ACOP action also extends to elevate other pains including migraine and muscular aches, neuralgia, back and rheumatic pain, and protects against ovarian cancer [1-6]. It was reported that very few or almost no side effects are suffered by patients treated with ACOP [7, 8].

The development of voltammetric sensors for the determination of catecholamine neurotransmitters (NTs) including dopamine (DA) has received considerable interest during the last few years [9]. Other NTs of interest are levodopa (L-DOPA), serotonin (ST) and norepinephrine (NEP). Trace level measurements in the brain are especially important in studying the role of NTs in neuro-physiology and disease control.The change in the level of NTs have been associated with various diseases and disorders, such as Parkinson's disease [10], Alzheimer's disease [11], Down's syndrome, Huntington's disease [12], schizophrenia, epilepsy and cocaine addiction [13]. The determination of these important biological molecules is therefore of prime importance to the medical field and pharmaceutical industry.

The chemical structure of room temperature ionic liquids (RTILs) contains mainly ions. Some interesting properties of RTILs rendered these materials useful in several applications such as high chemical and thermal stability, relatively high ionic conductivity, negligible vapor pressure and wider electrochemical windows [14]. Because of their relatively high ionic conductivity, electrode modification using RTILs was cited by several researchers in the last few years [15–18]. The enhanced ionic conduction is also advantageous to allow substituting ILs for paraffin oil to construct carbon-based voltammetric electrodes. Electrocatalysis and several other enhancing properties proved effective when using carbon ionic liquid electrode (CILE) as probes in electrochemistry [19], gas and liquid chromatography [20], mass spectrometry [21], capillary electrophoresis [22] and other sensors [23-30]. The electrochemical behavior of electroactive molecules, such as clozapine, adenine, guanine, nitrite, dopamine, ascorbic acid and DNA were also investigated using IL modified electrodes [31–36].

Combining the unique properties of ionic liquids and liquid crystals is realized in ionic liquid crystals (ILCs). These materials are anisotropic in nature that allows control of thermal behavior through ion exchange. This is in contrast to conventional mesogens that

often require tedious organic synthesis routes. The mesophase is developed and stabilized when ionic moieties are incorporated into the ILCs that distinguish their properties from regular ionic liquids. In general, lamellar mesophases are favored because of the distinct segregation between ionic and non-ionic parts and cation-anion pairing. One of the most promising features of ionic liquid crystals is ionic conductivity that will widen their application as ingredient in fabrication of electrode materials.

Nanostructured materials have also been used extensively as modifiers for electrochemical sensors for the analysis of environmental, biological, and pharmaceutical samples [41–44]. Nano-materials provide enhanced electron transfer, large edge plane/basal plane ratios, and rapid kinetics of electrode processes [45–48]. Metal oxide nanoparticles such as nickel oxide have been successfully used for immobilization and direct electrochemistry of biomolecules [49]. Research on the synthesis of nanosize porous nickel oxide materials and its applications in catalytic reactions and in industrial applications was mentioned in previous publications [50–52]. Furthermore, due to the excellent electrocatalytic activity and good antifouling properties of electrodes modified with nickel oxide, these modified electrodes have been used for enhanced oxidation and determination of insulin, thiols, disulfides, mercaptans, and sulfur oxoanions [53–55].

Surfactants are amphiphilic molecules with hydrophilic head and a long hydrophobic tail. Surfactants adsorb on the electrode surface and affect the electrode/electrolyte interactions. The interactions at the interface affect the electrochemical processes of electroactive analytes [56, 57]. Thus several applications were reported for these compounds in electrochemistry and electroanalytical studies [58]. Also, they have proven effective in the electroanalysis of some biological compounds and drugs [59–62]. Surfactants were suggested to combine with the substrate and results in their adsorption on the electrode surface, which facilitated the electron or the substance transfer between the electrode and the solution [63–66].

In this work, for the first time we introduce a new composite based on nickel oxide nanoparticles and ionic liquid crystal in presence of SDS (NiONps/ILCMCPE…..SDS) for determination of paracetamol (ACOP) and neurotransmitters compounds. The voltammetric response of the composite towards the electrooxidation of these compounds will be compared with composites based on nickel oxide nanoparticles and ionic liquids

in presence of SDS (NiONps/ILMCPE…..SDS). The sensor will be tested for its stability and anti-interference ability via the simultaneous determination of ACOP/DA and selective determination of ACOP in presence of AA and UA. Furthermore the sensor will be applied for direct determination of ACOP in human urine samples and for the drug assay in pharmaceutical formulations. This work will allow comparing the solid/solid interaction between ILCs and carbon-based structures to the liquid/solid interaction of ILs and carbon materials.

2. Experimental

2.1. Chemicals and Reagents

All chemicals were of analytical grade and used without any further purification. Acetaminophen (ACOP), ascorbic acid (AA), uric acid (UA), dopamine (DA), norepinephrine (NEP), levodopa (L-DOPA), serotonin (ST), the ionic liquid crystal (1-Butyl-1-methyl piperidinium hexafluoro phosphate), ionic liquids (1-n-Hexyl-3-methyl imidazolium tetrafluoroborate) (ILMCPE1) and (1-Butyl-4-methyl pyridinium tetrafluoroborate) (ILMCPE2), nickel oxide nanoparticles (NiONps) and sodium dodecyl sulfate (SDS) were purchased from sigma. The two ionic liquids are different in the nucleus of each (one is imidazolium based and the other is pyridinium based). Phosphoric acid and sodium hydroxide were purchased from (Adwic Co., Egypt), acetic acid was provided from Loba-Chemic Co., India, and boric acid from Polski Chemiczne, Poland) The chemicals were used without further treatment or purification. Britton-Robinson buffer (B-R buffer) was prepared by mixing different volumes of 0.04 M H_3PO_4, 0.04 M acetic acid and 0.04 M boric acid with the appropriate amount of 0.2 M NaOH to obtain the desired pH (2.0 - 9.0). Buffer solutions were kept in a refrigerator. All solutions were prepared from analytical grade chemicals and sterilized Milli-Q deionized water.

2.1.1. Preparation of bare CPE

Carbon paste electrode (CPE) was prepared by mixing graphite powder (0.5 g) with Nujol oil (0.3 mL) in a glassy mortar. The carbon paste was packed into the hole of the electrode body (with 5.6 mm inner diameter) and smoothed on a filter paper until its shiny appearance.

2.1.2. Preparation of modified CPEs

Carbon paste electrode modified with ionic liquid crystal (1-Butyl-1-methylpiperidinium hexafluorophosphate) was prepared by mixing 1.5 g of graphite powder, 0.5 g ILC with 0.5 ml of mineral oil (Nujol) in a mortar with a pestle to form a homogeneous paste. NiONps were incorporated to the paste by 1% (w/w) in a mortar and pestle for 30 min. Then the resulting paste was packed firmly in the hole of the electrode body. The electrode (ILCMCPE) was rinsed with water to remove any non-adsorbed modifier and dried in air at room temperature. The two other ionic liquid modified carbon paste electrodes (ILMCPE) were prepared following the same procedure; by mixing ILs (1-n-Hexyl-3-methyl imidazolium tetrafluoroborate) or (1-Butyl-4-methyl pyridinium tetrafluoroborate) to graphite powder with a ratio of 1% (w/w) and NiONps. All experiments were performed in presence of 10 µl of 0.01M SDS.

2.2. Instrumental and experimental set-up

2.2.1. Electrochemical measurements

Voltammetric measurements were performed using an electrochemical workstation AEW2 (Sycopel Scientific, England). The data were analyzed using ECprog3 electrochemistry software. A one-compartment cell was used with 2 cm^2 platinum electrode and 3M Ag/AgCl reference electrode. The glass electrochemical cell (15 mL) is fitted with gas bubbler for oxygen-deaeration. Experiments were conducted at room temperature under controlled atmosphere (25 °C). Solutions were degassed using pure nitrogen prior and throughout the electrochemical measurements.

The solutions pHs were measured using a JENWAY 3510 pH meter (England) connected to a glass combination electrode. Scanning electron microscopy (SEM) measurements were carried out using a field emission FE-SEM (JEOL JSM-6360LA electron microscope). Energy dispersive analysis of X-ray (EDAX) was used to identify the elemental composition of the surface.

2.2.2. Impedance spectroscopy measurements

Electrochemical impedance spectroscopy was performed using a Gamry-750 system and a lock-in-amplifier that are connected to a personal computer. The data analysis software was provided with the instrument and applied non-linear least square fitting with Levenberg-Marquardt algorithm. The parameters in electrochemical impedance experiment were as follows: different DC potential values of the corresponding oxidation

peak potential for each electrode was used (E_{pa}, as indicated in Table 3) at frequency range of 0.1–100000 Hz with an AC signal amplitude of 5 mV, was applied on bare CPE, ILCMCPE, NiONps/ILCMCPE and NiONps/ILCMCPE…..SDS which were tested in 1.0 × 10^{-3}M ACOP in B-R buffer (pH 7.4). The applied dc potential was determined from the cyclic voltammetry diagrams.

2.3. Analysis in spiked urine

Urine samples were obtained from healthy volunteer without any pretreatment, and were diluted 400 times with B–R buffer (pH 7.4) to eliminate matrix background effect. Standard ACOP provided by the National Organization for Drug Control and Research of Egypt was dissolved in B-R buffer pH 7.4 to make a stock solution with 1.0 × 10^{-3} M concentration. Successive additions of ACOP were added to 5 mL of diluted urine. The calibration graphs were constructed by plotting the peak current against drug concentration.

3. Results and discussion

Composite electrodes are fabricated as indicated in the experimental section based on nickel oxide nanoparticles and ionic liquid crystal in presence of SDS (in solution) (NiONps/ILCMCPE…..SDS). The electrochemical behavior of the proposed electrode will be studied and used for the determination of paracetamol (ACOP) and neurotransmitters compounds. A comparison will be also given between the proposed electrode and composite electrodes based on nickel oxide nanoparticles and ionic liquids in presence of SDS (NiONps/ILMCPE…..SDS). Two types of ionic liquids will be tested (1-n-Hexyl-3-methyl imidazolium tetrafluoroborate) (ILMCPE1) and (1-Butyl-4-methyl pyridinium tetrafluoroborate) (ILMCPE2). Other important parameters will be shown for the performance of the proposed sensor including surface morphological data.

3.1. Cyclic voltammetry of ACOP at the modified electrodes

The electrochemical behavior of 1.0 × 10^{-3} mol L^{-1} ACOP was studied using four different working electrodes (CPE…SDS, NiONps/ILMCPE1....SDS, NiONps/ILMCPE2...SDS and NiONps/ILCMCPE….SDS (the dots indicate that SDS is present in solution and not immobilized on the surface of the electrode). The cyclic voltammetry was measured in the range -100 to 800 mV in presence of 10 µL of 0.01 M SDS (figure 1) in B-R buffer pH 7.4, at a scan rate 100 mVs^{-1}. The anodic peak currents

for electrochemical oxidation of ACOP at bare CPE and at CPE in presence of 10 μL of 0.01 M SDS (CPE….SDS) were 45 μA and 51 μA respectively at oxidation potential 0.470 V.

The inclusion of NiONps should enhance the charge transfer rate regarding its catalytic properties [49-55]. Modification with ILCs should further enhance the current signal of the oxidation by increasing the ionic conductance within the electrode material. The electrochemical oxidation of ACOP was examined using cyclic voltammetry at different modified electrodes. At NiONps/ILMCPE1…..SDS and NiONps/ILMCPE2…..SDS, the oxidation peak currents were 63 μA and 69 μA, respectively. The oxidation potential was shifted to more positive value 0.525 V for NiONps/ILMCPE1…..SDS. Oxidation peak potential is 0.470 V at the NiONps/ILMCPE2…..SDS electrode compared to CPE. At NiONps/ILCMCPE…..SDS, anodic peak current of 115 μA (at 0.425 V) was obtained which is nearly two and half times higher than that obtained at bare CPE with negative shift of the oxidation potential value compared to NiONps/IL modified electrodes. The variation in the oxidation potential values illustrates the thermodynamic limitation with respect to each surface used in the electrochemical experiment.

Some ionic materials are also known to form amphitropic liquid crystals. Piperidinium salts for example have wider electrochemical potential window compared to the imidazolium and piperidinium analogues. The piperdinium salt deprotonate while keeping a localized positive charge on the nitrogen atom and on the aromatic ring for the other two salts. It will be advantageous to know that ILCs form ordered structures even in the solid state [67, 68]. A remarkable increase in the rate of electron transfer in such a system is expected that is due to the high polarizability and conductivity of ILCs [69, 70]. Another reason is the electrocatalytic activity of transition metal ions, electronic conductivity and good antifouling properties of electrodes modified with nickel oxide nanoparticles [71]. ACOP is also expected to be in ionic form and the presence of SDS would therefore synergistically improve the current signal as the accumulation and preconcentration of electrolyte increases at the interface.

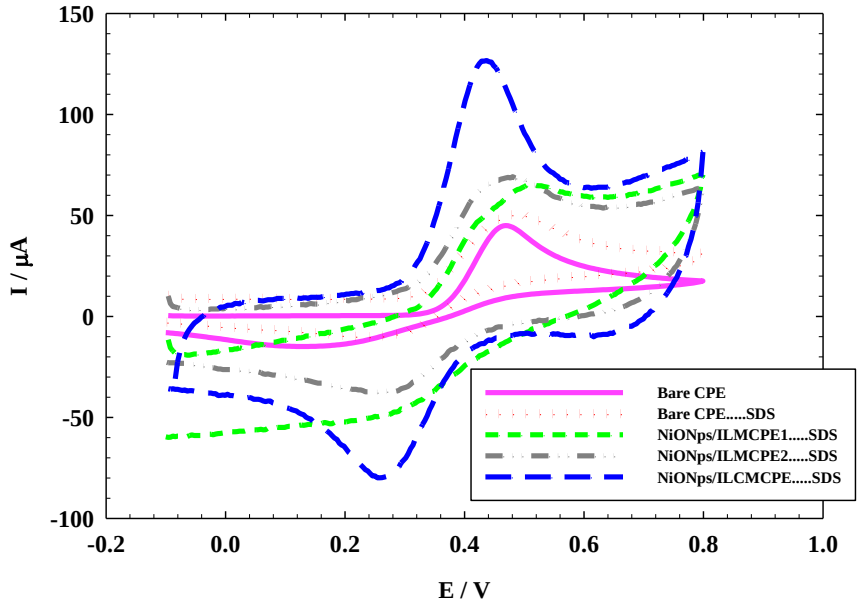

Figure 1. Cyclic voltammograms (CV) of 1.0 x 10^{-3} mol L^{-1} of ACOP in B-R buffer pH 7.4 at scan rate 100 mVs^{-1} recorded at different working electrodes (bare CP (solid line), Bare CPE…..SDS(dotted line), NiONps/ILMCPE1…..SDS (small dashed dotted line) , NiONps/ILMCPE2…..SDS(dashed dotted line) and NiONps/ILCMCPE…..SDS (large dashed line).

3.2. Electrochemical impedance spectroscopy (EIS) studies

Since the major contribution to the enhancement of charge transfer is attributed to surface rearrangements, EIS helps understanding the interfacial properties of surface modified electrodes. Therefore, EIS was used to investigate the nature of ACOP interaction at NiONps/ILCMCPE…..SDS surface in comparison to other electrode surfaces. EIS data are obtained for the modified electrode at ac frequency varying between 0.1 Hz and 100 kHz with an applied potential according to the oxidation potential values (E_{pa}) as indicated in table 3 (for each electrode) (vs. Ag/AgCl) in the region corresponding to the electrolytic oxidation of 1.0 mmol L^{-1} ACOP in 0.04 M B-R buffer pH 7.4. Fig. 2A shows a typical impedance spectrum presented in the form of Nyquist plot of ACOP at CPE, ILMCPE, NiONps/ILMCPE and (inset) NiONps/ILCMCPE…..SDS. The experimental data were compared and fitted to an equivalent circuit according to the non-linear least square fitting with Levenberg-Marquardt algorithm (the goodness of the fitting was verified according to the Kramers-Kronig fit). The circuit used some of the

conventional circuit elements, namely; resistance, capacitance, diffusion, and constant phase elements. The equivalent circuit is shown in fig. 2B. In this circuit, Rs is the solution resistance, R_{ct} is the charge transfer resistance (that will be affected by changes in the interface), R_f is the film resistance (that will be affected by the inclusion of ILC and nanostructures). Capacitors in EIS experiments do not behave ideally; instead they act like a constant phase element (Yo). Therefore, (Yo1) is a constant phase element representing surface roughness and (a) is its corresponding exponent (a is less than one). C_f is the film capacitance and C_{dl} represents the capacitance of the double layer. Diffusion can create impedance known as the Warburg impedance W (a constant diffusion parameter is considered in this case and assuming that diffusion within the film will also be affected by interfacial changes.

Table 1 lists the best fitting values calculated from the equivalent circuit for the impedance data. The error analysis is: $\chi^2 = 3.48 \times 10^{-3}$, the weighed sum of squares = 1.27×10^{-2} and the goodness of fit is 1.048×10^{-3}. The NiONps/ILCMCPE…..SDS shows increased values of the interfacial capacitance component compared to the other electrodes due to increase in ionic accumulation at the surface of the electrode. The value of R_{ct} decreases in the interfacial electron transfer region which is attributed to the selective interaction between NiONps/ILCMCPE…..SDS and ACOP. Good electronic and ionic conductivity of NiONps/ ILCMCPE…..SDS resulted in the observed increase in the current signal for the electro-oxidation process. An important feature in the data is the decrease in the value of film resistance (R_f) that ascertain the ionic conductance increase upon ILC inclusion and due to the increase in the metallic character imparted by nanostructure presence in the film. The roughness factor represented by an increase in the value of Yo1 is noticed as the solid components increase in the structure.

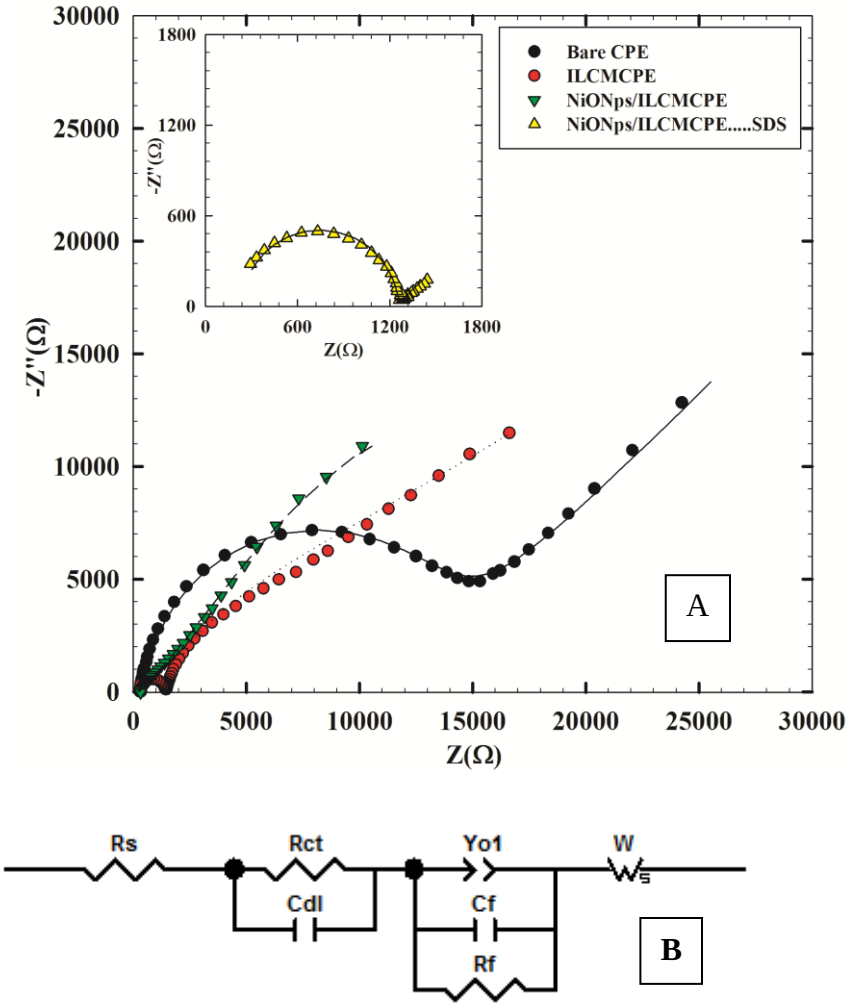

Figure 2. A) Typical impedance spectrum presented in the form of the Nyquist plot for Bare CPE (●), ILCMCPE (★), NiONps/ILCMCPE (■) and NiONps/ILCMCPE …..SDS (▼) against 1 mmol L^{-1} ACOP in BR buffer (pH 7.4). (Symbols and solid lines represent the experimental measurements and the simulation fitting of impedance spectra, respectively).**B)** Equivalent circuit used in the fit procedure of the impedance spectra.

	E_{pa} (mV)	Rs (kΩ cm^2)	Rct (kΩ cm^2)	C_{dl} (μF cm^{-2})	R_f (Ω cm^2)	C_f (μFcm^{-2})	W (kΩ $S^{-1/2}$)	Yo1 (S s^{a/cm^2})	a
Bare CPE	470	0.258	1.61	1.13	14.6	0.146	15.7	0.124	0.18
ILCMCPE	482	0.252	0.641	1.20	6.41	2.17	7.11	0.819	0.33
NiONps/ILCMCPE	457	0.239	0.113	6.03	2.08	4.16	4.65	1.56	0.49
NiONps/ILCMCPE..SDS	425	0.198	0.100	6.12	1.27	6.72	2.13	7.88	0.75

Table 1. Electrochemical impedance spectroscopy fitting data corresponding to Fig 2 (A and B).

3.3 Morphologies of the different electrodes

The surface homogeneity and roughness affect the extent of adsorption and rate of charge transfer. Thus, scanning electron microscopy (SEM) was used to characterize the morphology of the bare CPE, ILCMCPE, NiONps/ILCMCPE and NiONps/ILCMCPE…..SDS. Figure 3 represents the SEM morphology of the prepared electrodes. The SEM image of the bare carbon paste electrode (Fig.3A) showed edge-structured layering of graphite flakes. The surface structure of the bare carbon paste electrode also shows that the graphite particles are covered by a very thin film of paraffin oil which is not clearly shown because of lack of resolution. The SEM image of ILCMCPE (Fig 3B) exhibits clearly observed roughness increase that should result in relatively larger surface area. This could be attributed to the high viscosity of ILC used, which infiltrated into the void space between the graphite flaks. Figure 3C showed a microstructure with a continuous grain growth of nanoparticles incorporated with ILC in NiONps/ILCMCP. Also, a spongy film is observed in Fig. 3(D) due to the surfactant film on the surface which influences the conductivity level of the film and helps the attraction of ACOP to the electrode surface. It is worth mentioning that the scale of the SEM images differed in order to reveal the structural details for each surface. In addition, the energy dispersive X-ray (EDX) spectra of NiONps/ILCMCPE…..SDS confirmed the presence of NiONps in the paste as shown in Figure 4.

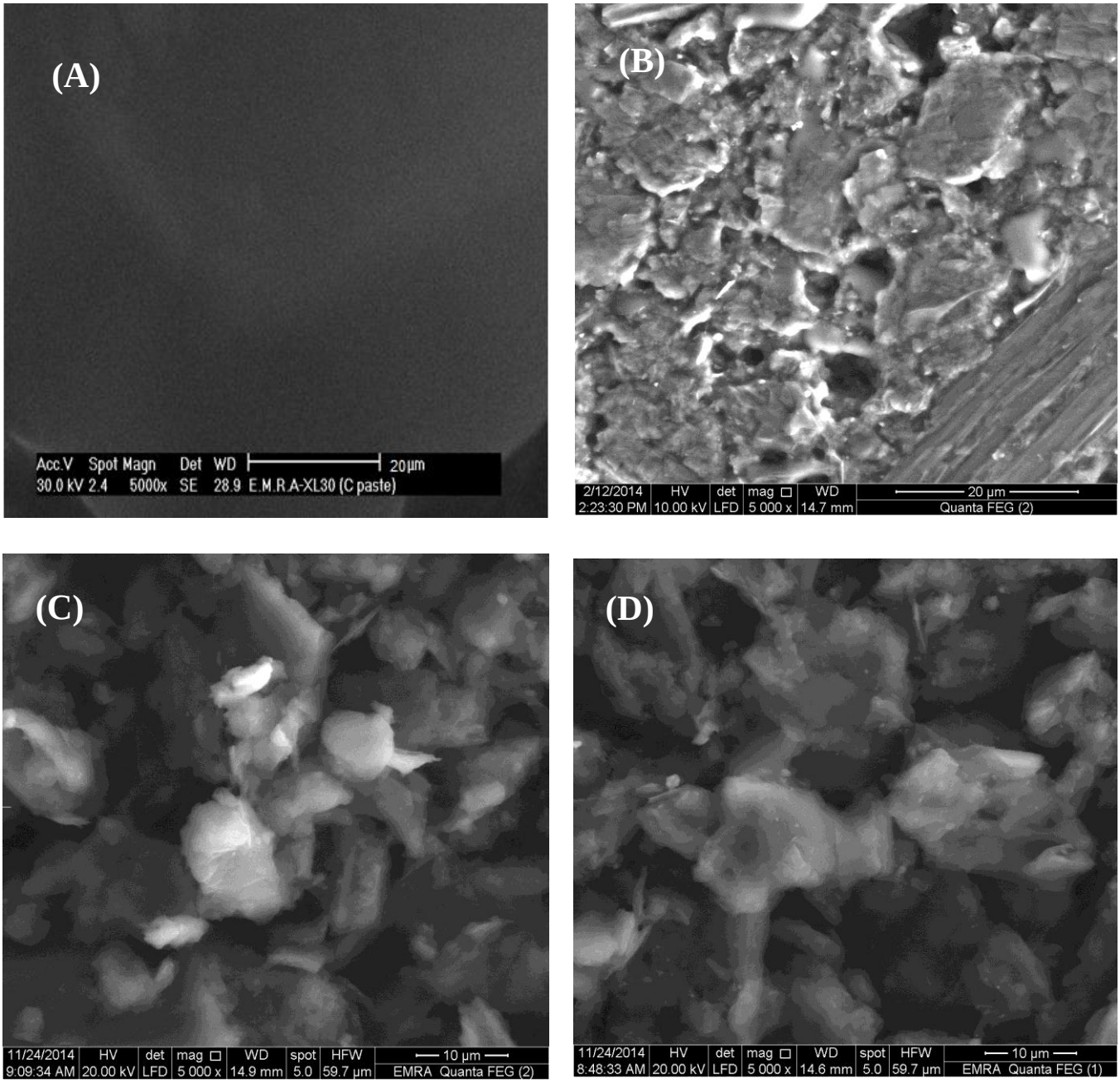

Figure 3. Scanning electron microscope of different electrodes: A) Bare CPE, B) ILCMCPE, C) NiONps/ILCMCPE and D) NiONps/ILCMCPE…..SDS.

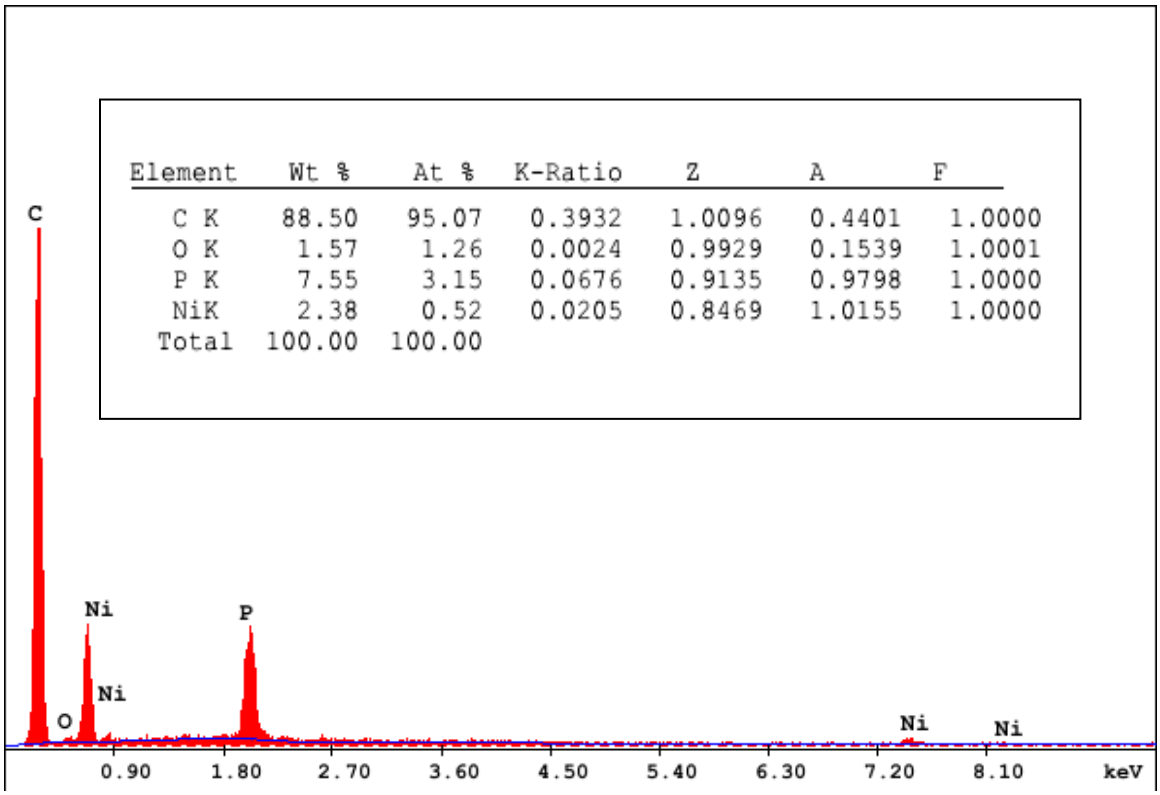

Figure 4. EDX spectra obtained from NiONps/ILCMCPE…..SDS.

3.4. Electrochemistry of ACOP and neurotransmitters

The voltammetric behavior of ACOP and some neurotransmitters (DA, NEP, ST and L-Dopa) were examined at bare CPE, bare CPE…..SDS, ILCMCPE, ILCMCPE…..SDS, NiONps/ILCMCPE and NiONps/ILCMCPE…..SDS using cyclic voltammetry. Table 2 summarizes the electrochemical data for the oxidation of the studied compounds. Upon modification with NiONps/ILCMCPE…..SDS, the oxidation peak current increased and the oxidation potential shifted to less positive values due to the improvements in the reversibility of the redox reaction and facilitation of the electron transfer process at the modified electrode. The thermodynamic limitation is realized in lower oxidation potential values and kinetically enhanced as manifested by the increase in the current values. Figure 5 shows typical cyclic voltammograms of 1.0 mM (A) ACOP, and (B) one of the neurotransmitters (L-Dopa), in B–R buffer pH 7.4 at scan rate 100 mV s^{-1} recorded at bare CPE (solid line), CPE…..SDS (dotted line), ILCMCPE (small dashed line),

ILCMCPE…..SDS (dashed double dotted line), NiONps/ILCMCPE (large dashed line) and NiONps/ILCMCPE…..SDS (dashed dotted line). The incorporation of NiONps into ILCMCPE in presence of SDS resulted in an observable increase in the peak current, which indicated an improvement in the electrode kinetics and a decrease in the potential of oxidation substantially (i.e. thermodynamically feasible reaction) in all the compounds studied compared to the bare CPE. The results confirmed the key role played by NiONps, ILC and SDS on the catalytic oxidation, which enhances the electrochemical reaction as discussed earlier. IL incorporation resulted in an increase in the conductivity that is relatively less pronounced compared to ILC. At this stage it could be concluded that surface alignment of ILCs proved effective in this application.

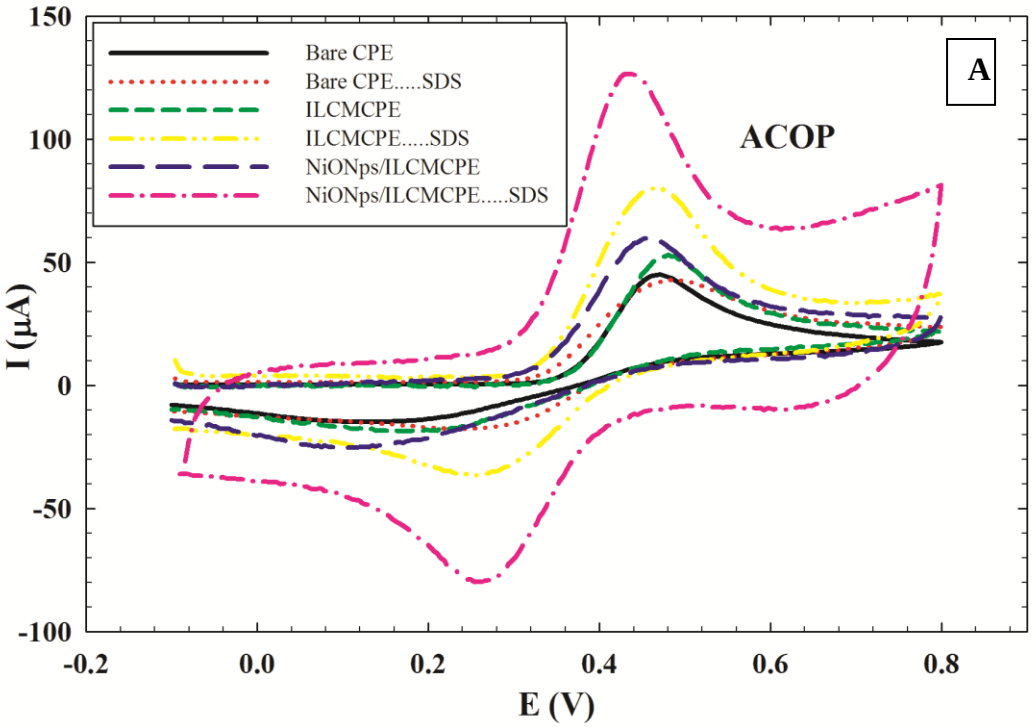

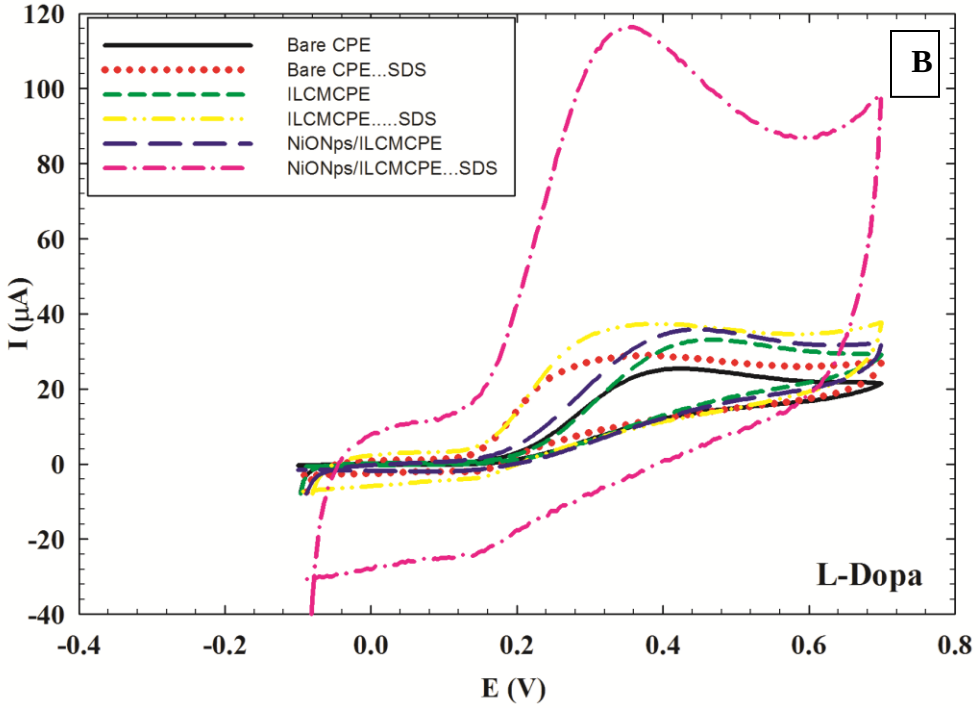

Figure 5. (**A**) Cyclic voltammograms of 1.0 mM ACOP in B–R buffer pH 7.4 at scan 100 mV s^{-1} recorded at Bare CPE, Bare CPE…..SDS, ILCMCPE, ILCMCPE…..SDS, NiONps/ILCMCPE and NiONps/ILCMCPE…..SDS. (**B**) Cyclic voltammograms of 1.0mM L-Dopa in B–R buffer pH 7.4 at scan rate100 mV s^{-1} recorded at Bare CPE, Bare CPE…..SDS, ILCMCPE, ILCMCPE…..SDS, NiONps/ILCMCPE and NiONps/ILCMCPE…..SDS.

	ACOP		DA		L-DOPA		ST		NEP	
	I(µA)	E(mV)	I(µA)	E(mV)	I(µA)	E(mV)	I(µA)	E(mV)	I(µA)	E(mV)
Bare CPE	45	472	13	379	12	412	17	435	23	414
Bare CPE…..SDS	51	472	43	232	29	374	36	387	15	270
ILCMCPE	53	482	25	304	34	445	37	417	38	404
ILCMCPE….. SDS	80	464	65	252	37	386	60	401	17	264
NiONps/ILCMCPE	60	457	32	312	36	445	32	425	11	329
NiONps/ILCMCPE …..SDS	115	425	111	257	102	339	100	417	98	363

Table 2. Summary of CV results obtained at Bare CPE, Bare CPE…..SDS, ILCMCPE, ILCMCPE…..SDS, NiONps/ILCMCPE and NiONps/ILCMCPE…..SDS for 1 mmol L^{-1} of each compound in BR buffer pH 7.4.

3.5. Parameters affecting the electrode performance

3.5.1. Effect of varying the solution pH

The effect of solution pH on the electrocatalytic oxidation of ACOP and the neurotransmitters at NiONps/ILCMCPE…..SDS were studied by cyclic voltammetry in Britton–Robinson buffers within the pH range of 2–9 (figure 6A). The pH of solution has a significant influence on the peak potential of the catalytic oxidation of ACOP. It is noticed that the anodic peak potentials shifted negatively with the increase of the solution pH, indicating that the electrocatalytic oxidation at the NiONps/ILCMCPE…..SDS is a pH dependent reaction. Protons therefore take part in the electrochemical process. The highest current response was obtained at pH 2 and pH 7. Also, the peak potential for ACOP oxidation varies linearly with pH (over the pH range from 2 to 9). The dependence of Epa on pH at the NiONps/ILCMCPE…..SDS can be expressed by the relation:

Epa (V) = 0.786-0.052pH (vs. Ag/AgCl) with a coefficient of 0.9999.

The slope was found to be -52.0 mV/pH-unit over the pH range from 2 to 9, compared to the theoretical value of −59 mV. This indicates that the number of protons and electrons involved in the oxidation mechanism is equal. The current response was also affected by changing the pH of the medium, thus, Figures 6B and 6C show the graph of current response of some neurotransmitters and ACOP, at different pH values at bare CPE and NiONps/ILCMCPE…..SDS, respectively. It is clear that at NiONps/ILCMCPE…..SDS the anodic current responses for all neurotransmitter compounds and ACOP through the whole pH range are higher than the values obtained at bare CPE.

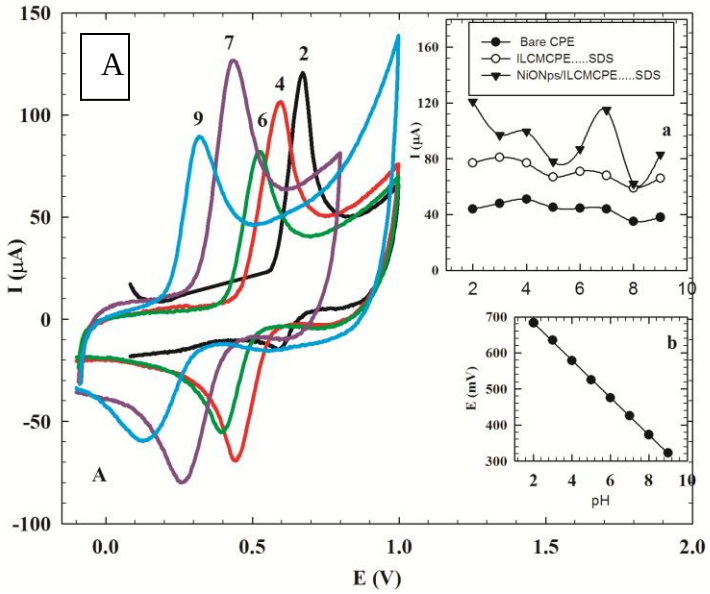

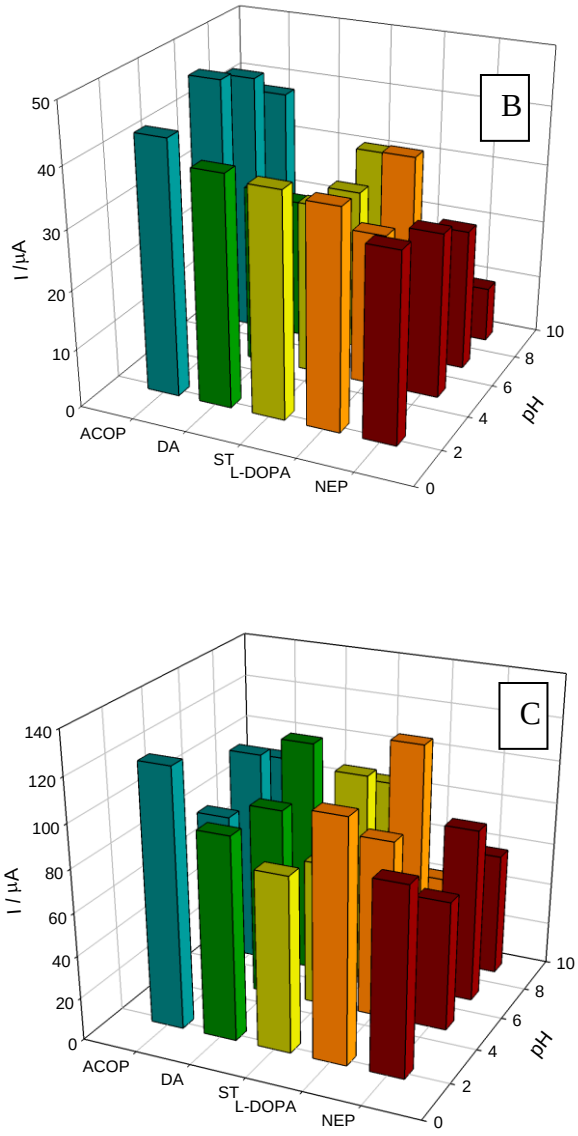

Figure 6. A) Cyclic voltammetric response of 1.0 mmol L^{-1} ACOP at NiONps/ILCMCPE…..SDS in 0.04 M B-R buffers of different pH values (2-9).inset (a): Comparison between the anodic peak currents at different pH values of Bare CPE (●), ILCMCPE …..SDS (■) and NiONps/ILCMCPE…..SDS (▼).inset (b): The anodic peak potentials at NiONps/ILCMCPE…..SDS at different pH values. **B**) A graph of current response of some neurotransmitters and ACOP, at different pH values, at the Bare CPE. **C**) A graph of current response of some neurotransmitters and ACOP, at different pH values, at NiONps/ILCMCPE…..SDS.

3.5.2. Effect of the scan rate

The effect of different scan rates (ν ranging from 10 to 250 mV s^{-1}) on the current response of ACOP and one of the neurotransmitters (DA) (1.0×10^{-3} M) on NiONps/ILCMCPE…..SDS in B–R buffer (pH 7.4) were studied and a plot of peak current (i_{pa}) versus the square root of the scan rate ($\nu^{1/2}$) gave a straight line relationship. This revealed that the linearity of the relationship was realized up to a scan rate of 250 mV s^{-1}. This indicated that the charge transfer was under diffusion control. Typical CV curves of ACOP and DA at different scan rates are shown in Fig. 7A and 7B respectively. The peak-to-peak separation also increased with increasing the scan rate. A good linear relationship was found for the oxidation peak currents, with different scan rates (inset of figures). The oxidation peak currents increased linearly with the linear regression equations as:

i_{pa} (10^{-6} A) = -15.707 $\nu^{1/2}$ (V s^{-1})$^{1/2}$ + 35.333 (n = 7, γ = 0.9985) and i_{pa} (10^{-6} A) = -14.497 $\nu^{1/2}$ (V s^{-1})$^{1/2}$ + 31.099 (n = 7, γ = 0.9972) for ACOP and DA , respectively.

This suggests that the electrode reaction is under diffusion control.

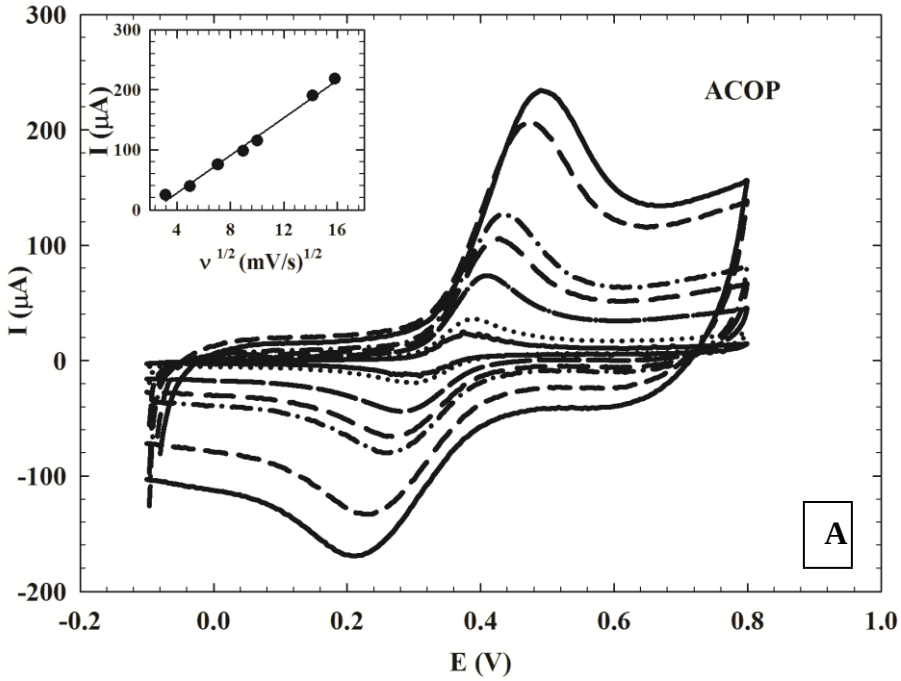

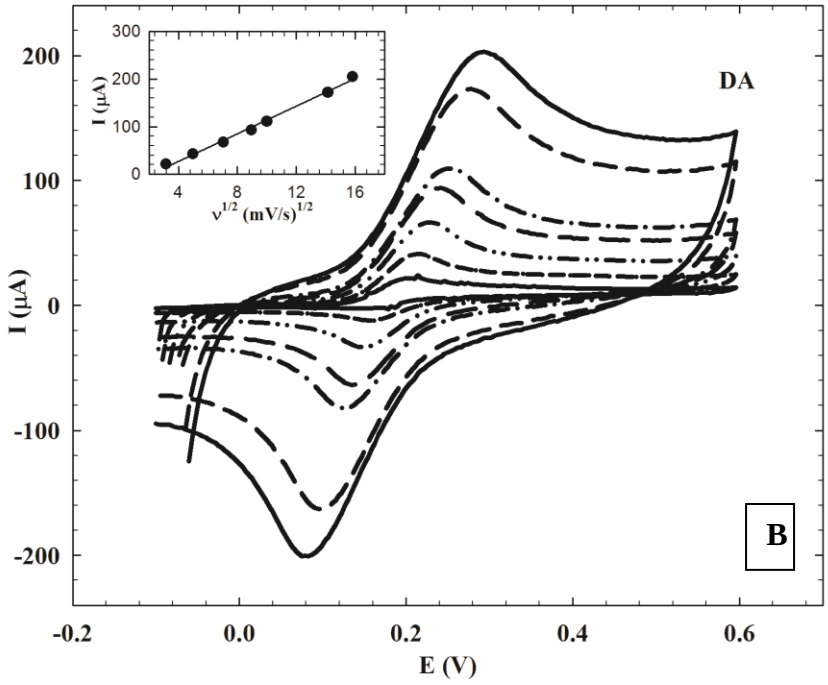

Figure 7. A) Cyclic voltammograms (CV) of 1.0 x 10^{-3}M ACOP at the NiONps/ILCMCPE…..SDS in 0.04 M B–R buffer pH 7.4 at: 10, 25, 50, 80, 100, 200 and 250 mV s^{-1}.Inset: plot of the anodic peak current values versus square root of scan rate. **B**) Cyclic voltammograms (CV) of 1.0 x 10^{-3}M DA at the NiONps/ILCMCPE…..SDS, in 0.04 M B–R buffer pH 7.4 at: 10, 25, 50, 80, 100, 200 and 250 mV s^{-1}.The inset: plot of the anodic peak current values versus square root of scan rate.

3.5.3. Diffusion coefficients of ACOP and NT compounds

The dependence of the anodic peak current density on the scan rate has been used for the estimation of the ‘‘apparent’’ diffusion coefficient, Dapp, for the compounds studied. Dapp values were calculated from the Randles Sevcik equation, and for the oxidized species [O]: (For T = 298 K at which temperature the experiments were conducted)

$Ip_a = (2.69 \times 10^5)\, n^{3/2} A C_0 D_0^{1/2} \nu^{1/2}$

Where the constant has the units: 2.687×10^5 C mol^{-1} $V^{-1/2}$. In these equations: Ip_a is the peak current density (A cm^{-2}), n is the number of electrons appearing in the half-reaction for the redox couple, ν is the rate at which the potential is swept (V s^{-1}), F is Faraday’s constant (96 485 C mol^{-1}), C_0 is the analyte concentration (1×10^{-6} mol cm^{-3}), A is the electrode area (0.0706 cm^2), R is the universal gas constant (8.314 J mol^{-1} K^{-1}), T is the absolute T/K, and D is the electroactive species diffusion coefficient (cm^2 s^{-1}).

Apparent surface area used in the calculations did not take into account the surface roughness. The apparent diffusion coefficients, D_{app}, of ACOP and the studied neurotransmitters on NiONps/ILCMCPE…..SDS in B–R buffer (pH 7.4) were calculated from cyclic voltammetry (CV) experiments and were in the range of (3.33×10^{-5}-4.58×10^{-5} cm^2 s^{-1}), these results were compared to those calculated in the case of bare CPE, which were in the range of (4.99×10^{-7} -7.02×10^{-6} cm^2 s^{-1}), as shown in Fig. 8. This graph indicated the fast mass transfer of the analyte molecules towards the NiONps/ILCMCPE…..SDS surface from bulk solutions and/or fast electron transfer process of electrochemical oxidation of the analyte molecule at the electrode solution interface [72, 73]. Furthermore, it also showed that the redox reaction of the analyte species took place at the surface of the electrode under the control of the diffusion of the molecules from solution to the electrode surface. The calculated D_{app} values at the bare CPE and NiONps/ILCMCPE…..SDS showed that NiONps, ILC and SDS improve the electron transfer kinetics at the electrode/solution interface.

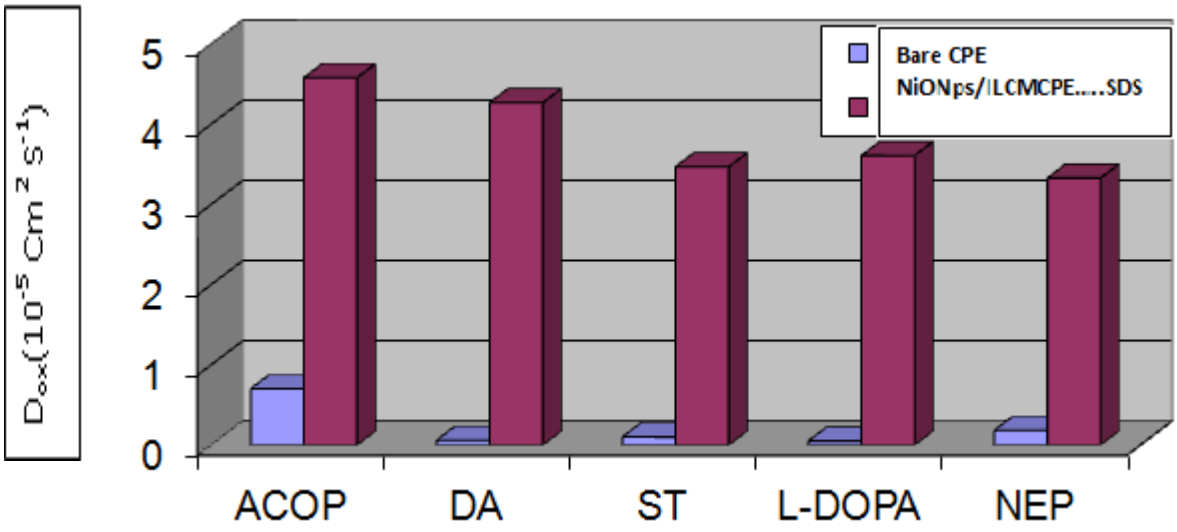

Figure 8. A graph indicating the apparent diffusion coefficients, D_{app}, of ACOP and the studied neurotransmitters at NiONps/ILCMCPE…..SDS and Bare CPE.

3.6. Effect of interferences on the behavior of ACOP

In biological samples, AA and UA are the common important interferences for the determination of neurotransmitters at sensor surfaces. To check the sensitivity and

selectivity of the sensor in the presence of these interferences, the NiONps/ILCMCPE…..SDS was used for voltammetric detection of ACOP in presence of AA and UA. Mixture (I) contains 1.0 mM AA, 1.0 mM UA and 1.0 mM ACOP in B-R buffer pH 7.4, the applied scan rate was 10 mV/s using differential pulse mode. Fig 9-curve AI shows the differential pulse voltammograms obtained with the Bare CPE (dashed line) and NiONps/ILCMCPE…..SDS (solid line) in 1 mmol L^{-1} UA. The current response at the CPE was 43.1 μA and decreased to 11.4 μA at the NiONps/ILCMCPE…..SDS (solid line). The determination of 1.0×10^{-3} mol L^{-1} AA on bare CPE (dashed line) gives a peak current of 22.7 μA which disappears using NiONps/ILCMCPE…..SDS (solid line) (curve AII).

Curve AIII shows that the anodic peak current of 1.0×10^{-3} mol L^{-1} ACOP increased from 25.04 μA in case of Bare CPE (dashed line) to 52.67 μA using NiONps/ILCMCPE…..SDS (solid line). Curve B shows the voltammograms of mixture (I), under the same optimum experimental conditions. As can be noticed in case of Bare CPE (dashed line) only one peak for UA, AA and ACOP has been obtained, while in case of NiONps/ILCMCPE…..SDS (solid line) one sharp peak with relatively higher peak current for ACOP at 365 mv and a second peak for uric acid were observed as illustrated in Fig 9B.

The results of this study show that it is possible to determine ACOP selectively in presence of high concentration of AA and UA by using the proposed modified electrode. Other interference studies are given in supplement 3 for serotonin, norepinephrine and L-Dopa.

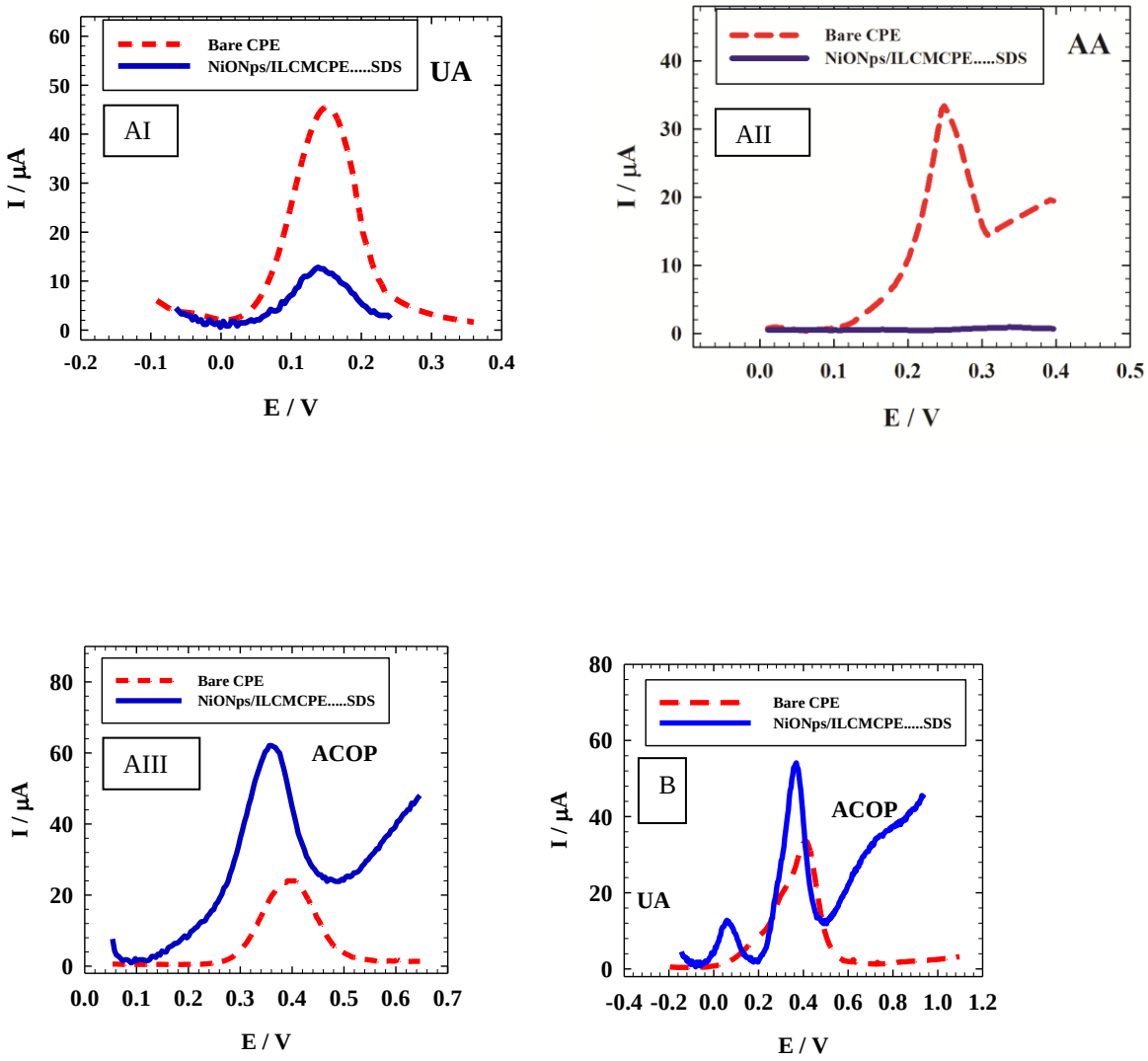

Figure 9. A) The differential pulse voltammograms obtained with the Bare CPE(dashed line) and NiONps/ILCMCPE…..SDS (solid line) of I) 1.0 mM UA, II) 1.0 mmole L^{-1} AA and III) 1 mmole L^{-1} ACOP, in 0.04 M B-R buffer pH 7.4, scan rate 10 mVs^{-1}. **B)** The differential pulse voltammograms obtained at Bare CPE (dashed line) and iONps/ILCMCPE…..SDS (solid line) for a mixture of 1.0 mmole L^{-1} ACOP + 1.0 mmole L^{-1} AA + 1 mmole L^{-1} UA in 0.04 M B-R buffer pH 7.4, scan rate 10 mV s^{-1}.

3.7. Simultaneous determination of ACOP and DA

It very important to determine ACOP in presence of neurotransmitter compounds which play important roles in various biological, pharmacological and physical processes in human body. Dopamine (DA) is one of the most important neurotransmitters that are widely distributed in the mammalian central nervous system for message transfer and it

plays a very important role in the functioning of central nervous system. As shown in Fig. 10A, ACOP exhibits well-defined differential pulse voltammograms DPV with good separations from DA in B-R buffer (pH 7.4) by changing the concentration of both ACOP (4.4-133.0 μmol L^{-1}) and DA (4.4-36.0 μmol L^{-1}). The current responses due to the oxidation of DA (at 170 mV) and ACOP (at 374 mV) with a peak separation of 204 mV were observed. With increasing their concentrations, the current responses of both ACOP and DA were increased linearly with a correlation coefficient of 0.9996 and 0.9981, respectively, also the regression equation for ACOP was found to be: Ip(μA) = 0.247 c(μmol L^{-1}) +4.951, while the regression equation for DA was : Ip(μA) = 0.832 c(μmol L^{-1}) + 5.748.

Simultaneous determination of ACOP and DA in the mixture was also investigated when the concentration of one species changed, whereas the other was kept constant. Figure10B showed that the peak current of ACOP increase with an increase in the ACOP concentration (8.89-89.0 μmol L^{-1}) while the concentration of DA was kept constant (4.4 μmol L^{-1}). Also keeping the concentration of ACOP constant (4.0 μmol L^{-1}), the oxidation peak current of DA was positively proportional to its concentration (4.44-44.11 μmol L^{-1}) (fig 10C).

It should be noted that, the change of concentration of one compound did not have significant influence on the peak current and peak potential of the other compound.

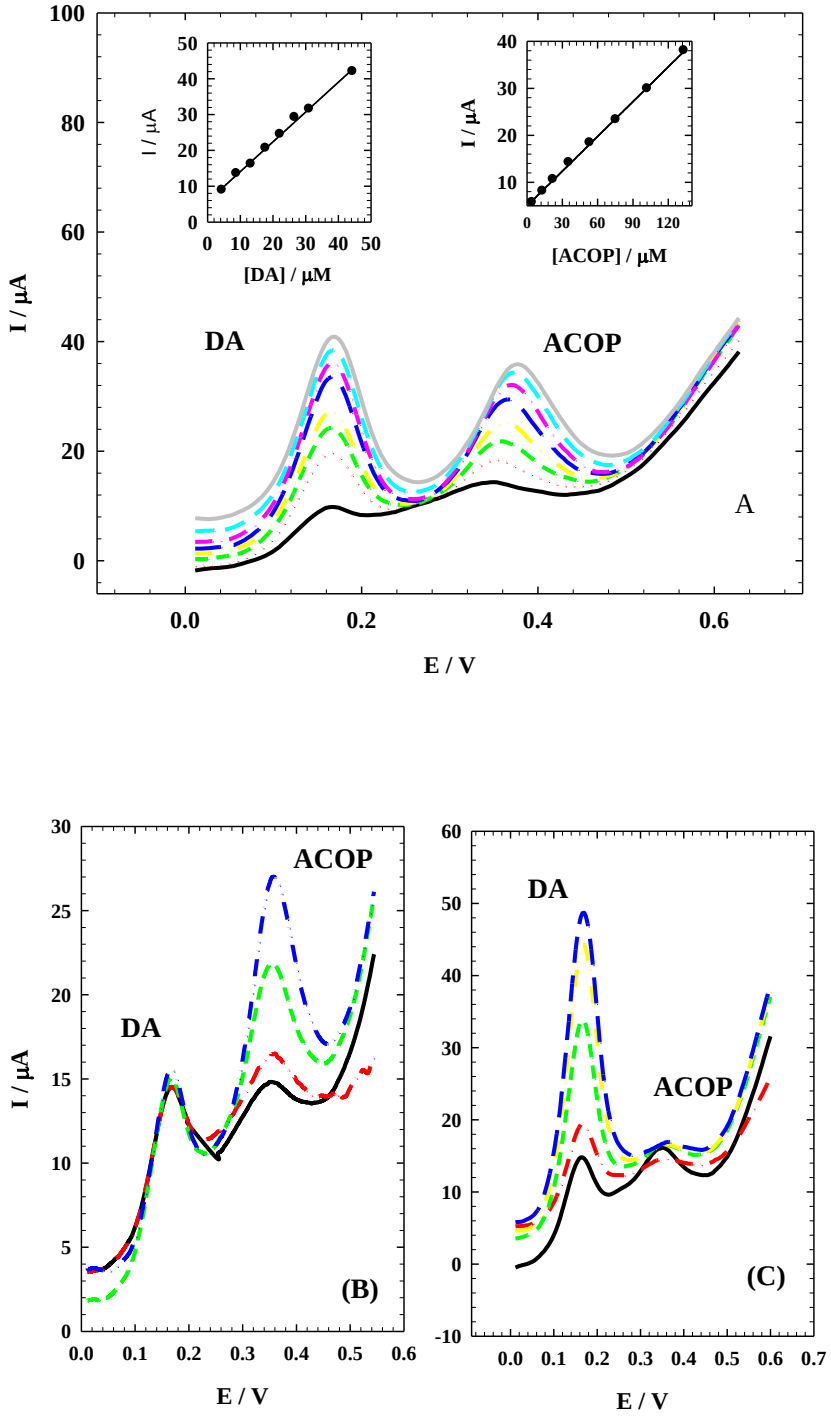

Figure 10. A) Differential pulse voltammograms at NiONps/ ILCMCPE…..SDS with good separations between ACOP and DA by changing the concentration of both ACOP (4.4→133.0 µmol L^{-1}) and DA (4.4→36.0 µmol L^{-1}) in 0.04 M B-R buffer pH 7.4, scan rate 10 mV/s. **B**) Differential pulse voltammograms at NiONps/ILCMCPE…..SDS, with

an increase in the ACOP concentration (8.89 → 89.0 µmol L^{-1}) while the concentration of DA was kept constant (4.4 µmol L^{-1}). **C**) Differential pulse voltammograms at NiONps/ILCMCPE…..SDS with increase in the DA concentration (4.44 → 44.11 µmol L^{-1}) while the concentration of ACOP was kept constant (4.0 µmol L^{-1}).

3.8. Analytical characterization of ACOP and reproducibility

Pulse voltammetric techniques, such as DPV, are effective and rapid electroanalytical techniques with well-established advantages, including good discrimination against background current and low detection limits. To prove the sensitivity of NiONps/ILCMCPE…..SDS towards the electrochemical measurement of ACOP, the effect of changing the concentration of ACOP in B–R buffer pH 7.4, using DPV mode was studied (Fig. 11). The following are the parameters for the DPV experiments: E_i = 100 mV, E_f = 600 mV, scan rate = 10 mV s^{-1}, pulse width = 25 ms, pulse period = 200 ms, and pulse amplitude = 10 mV. From the electrochemical responses in Figure 11, the calibration plots were linearly related to ACOP concentration over a relatively short linear range of 44.4 × 10^{-7} to 3.33 × 10^{-5} mol L^{-1} with a regression equation of I_p(µA) = 0.461 c(µM) + 5.951 and correlation coefficient 0.9997 and a large range of 5.56 × 10^{-5} to 2.78 × 10^{-4} mol L^{-1} with a regression equation of I_p(µA) = 0.081 c(µM) + 17.443 and correlation coefficient 0.9998.

The limits of detection (LOD) and the limits of quantitation (LOQ) were calculated from the oxidation peak currents using the following equations:

LOD = 3*s*/*m*

LOQ = 10*s*/*m*

Where *s* is the standard deviation of the oxidation peak current (three runs) and *m* is the slope (µAM^{-1}) of the related calibration curves and they were found to be 8.613 x10^{-9} mol L^{-1} and 2.871 × 10^{-8} mol L^{-1} for the small range and 5.680 × 10^{-8} mol L^{-1} and 1.893 × 10^{-7} mol L^{-1} for the large range respectively. Both LOD and LOQ values confirmed the sensitivity of NiONps/ILCMCPE…..SDS. Table 3 shows a comparison of the LOD of NiONps/ILCMCPE…..SDS with the reported different electrodes for the determination of paracetamol. Our work showed the lowest limit of detection compared to the other values mentioned in the literature using other modified electrodes. Table presented in supplement 4 shows a comparison between different techniques used for the

determination of acetaminophen and the present method. Beside the complication in preparing the samples and cost bearing with the other techniques presented in supplement 4, lower detection limits and better linear dynamic range is obtained using the proposed sensor in this work.

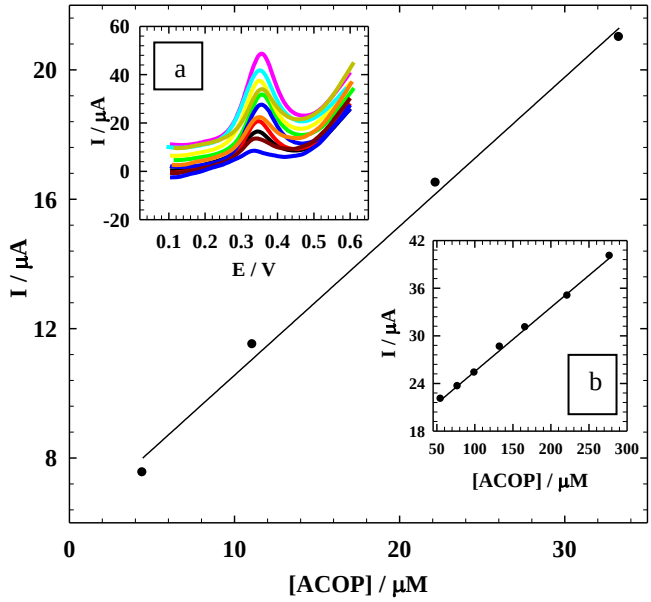

Figure 11. The calibration curve of smaller concentration range of ACOP.
Inset a: The effect of changing the concentration of ACOP, using DPV mode at NiONps/ILCMCPE…..SDS in 0.04 mole L^{-1} B-R buffer pH 7.4 and scan rate 10 mV/s.
Inset b: represents the calibration curve of the larger concentrations range.

Electrode used	Limit of Detection (LOD)	Ref. No.
Dipyrromethene-Cu(II) monolayers modified gold electrode	1.2×10^{-4} M	[74]
Carbon ionic liquid electrode	0.3×10^{-6} M	[75]
Nanogold modified indium tin oxide electrode	1.8×10^{-7} M	[76]
Fullerene modified glassy carbon electrode	5.0×10^{-5} M	[77]
Boron-doped diamond electrode	4.9×10^{-7} M	[78]
MWNT modified basal plane pyrolytic graphite electrode	1.0×10^{-8} M	[79]
CNT modified screen-printed carbon electrode	1.0×10^{-7} M	[80]
NiONps/ILCMCPE…..SDS	8.6×10^{-9} M	**This work**

Table 3. Comparison of the NiONps/ILCMCPE…..SDS with the reported different electrodes for the determination of (ACOP)

3.9. Validation in pharmaceutical and urine samples

The proposed sensor was validated for drug determination in formulation and urine according to the parameters described in the WHO technical report series [81]. From the pH study using the proposed electrode (section 3.5.1, Figure 6), a negative shift in oxidation potential of ACOP is observed as the pH increases. The highest current response was observed however at pH 7, and the method adopted was considered robust for this pH. The obtained validation results are described in Table S2 (Supplement 2). After the validation of the proposed sensor electrode, the tablets purchased from drug stores and urine samples spiked with ACOP were analyzed and the data are given in the following sections, respectively.

3.9.1 Validation in pharmaceutical samples

Commercial pharmaceutical samples (tablets) containing paracetamol was analyzed to evaluate the validity of the proposed method. Paracetamol tablets containing 500 mg ACOP were applied from SEDICO Pharmaceutical Company (Egypt). The tablets were weighed and finely pulverized. The appropriate amount of this powder was dissolved in double distilled water. The content of the tablet was diluted to obtain 1.0 mM of paracetamol and then DPV were recorded using NiONps/ILCMCPE…..SDS. The concentration of paracetamol in the pharmaceutical formulations was determined from the calibration curve. Average concentrations were calculated from five replicate measurements of two independent solutions of the same pharmaceutical preparations. Table 4 shows the data generated by standard addition method for the analysis of paracetamol in buffered solution of pH 7.4. The data shows that the content values determined by the proposed method for the commercial samples are very close to the claimed amount.

The analysis of the obtained responses allowed the conclusion that the drug excipients do not significantly interfere with the proposed method. Thus, the practical application was demonstrated with the determination of paracetamol directly in pharmaceutical formulations with satisfactory results. From Table 4 we can see that the recovery data obtained by the standard addition method for ACOP in drug formulations was found in

the range from 100.24% to 101.78% and the relative standard deviation (RSD) was in the range from 0.14% to 0.84%, suggesting that NiONps/ILCMCPE…..SDS has a high reproducibility and it would be a useful electrode for the quantitative analysis of ACOP in pharmaceutical formulations.

[Tablet] taken ($\times 10^{-6}$ M)	[Standard] added ($\times 10^{-6}$ M)	[Found] ($\times 10^{-6}$ M)	Recovery %	%RSD
5.0	5.00	10.110	101.10	0.35
10.0		15.260	101.73	0.21
20.0		25.060	100.24	0.14
30.0		35.108	100.31	0.34
50.0		55.980	101.78	0.84

Table 4. Recovery data obtained by the standard addition method for (ACOP) in drug formulation

3.9.2 Validation of the method in real samples of urine

Validation of the procedure for the quantitative assay of ACOP in urine was examined in B-R buffer pH 7.4, at scan rate 10 mV/s using DPV. The calibration curve (fig 12) gave a straight line in two linear dynamic ranges, the small range was from 4.54×10^{-6} mol L^{-1} – 2.67×10^{-5} mol L^{-1} with correlation coefficient, r = 0.9993, while the large range was from 4.44×10^{-5} mol L^{-1} – 1.89×10^{-4} mol L^{-1} with correlation coefficient, r = 0.9988. LOD was found to be 1.11×10^{-8} mol L^{-1} and 2.02×10^{-7} mol L^{-1} while LOQ was found to be 3.67×10^{-8} mol L^{-1} and 6.72×10^{-7} mol L^{-1} for small and large linear dynamic ranges respectively. Four different concentrations on the calibration curve are chosen to be repeated for five times to evaluate the accuracy and precision of the proposed method which is represented in (table-5). Also the recovery, standard deviation, standard error and the confidence level were calculated.

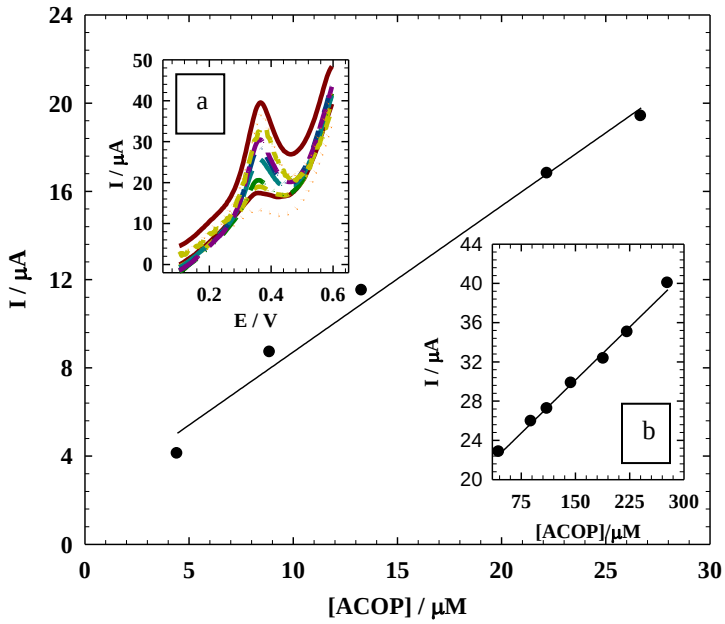

Figure 12. The calibration curve of smaller concentration range of ACOP. Inset a: The effect of changing the concentration of ACOP, using DPV mode at NiONps/ILCMCPE…..SDS in urine using 0.04M B-R buffer pH 7.4 and scan rate 10 mV s^{-1}. Inset b: represents the calibration curve of the larger concentrations range.

[ACOP] added (M) × 10^{-6}	[ACOP] Found[a] (M) × 10^{-6}	Recovery (%)	SD × 10^{-7}	S.E[b] × 10^{-7}	C.L.[c] × 10^{-7}
6.0	6. 12	102.0	0.83	0.48	2.06
10.0	10.1	101.0	2.64	1.18	3.28
25.0	25.6	102.5	3.22	1.86	3.98
50.0	49.8	99.6	2.09	0.85	2.20

[a]mean for five determinations
[b]Standard error = SD/√n
[c]C.L. confidence at 95%confidence level and 4 degrees of freedom (t=2.776)

Table 5. Evaluation of the accuracy and precision of the proposed method for the determination of ACOP in urine samples

4. Conclusion

In the present work, a novel sensor based on an ionic liquid crystal (1-Butyl-1-methyl piperidinium hexafluoro phosphate), nickel oxide nanoparticles and sodium dodecyl sulfate was used for the electrochemical determination of acetaminophen and some

neurotransmitters. Ionic liquid crystal (1-Butyl-1-methyl piperidinium hexafluoro phosphate), nickel oxide nanoparticles and sodium dodecyl sulfate enhanced the sensitivity of carbon paste electrode towards different compounds; furthermore, the ionic liquid crystal (1-Butyl-1-methyl piperidinium hexafluoro phosphate), nickel oxide nanoparticles and sodium dodecyl sulfate has been proved to be efficient for the electrocatalytic oxidation of paracetamol in biological fluids. Simultaneous determinations of acetaminophen with dopamine in a binary mixture were achieved with good separation. On the other hand, this sensor shows anti-interference ability; it can simultaneously determine acetaminophen with high current response in presence of large amount of ascorbic acid and uric acid and the method was simple, sensitive and successfully applied for determination of acetaminophen in human urine and in commercial tablets with good precision and accuracy. Under the optimum conditions, calibration plots for acetaminophen were linear in the ranges of 44.4×10^{-7} to 3.33×10^{-5} mol L^{-1} and 5.56×10^{-5} to 2.78×10^{-4} mol L^{-1} with correlation coefficients of 0.9997 and 0.9998 and detection limit of 8.613×10^{-9} mol L^{-1} and limit of quantitation 2.871×10^{-8} mol L^{-1} for small range. The good properties of this modified electrode will expand its application in electrochemical field for the determination of other drugs in biological fluids without any interference.

Acknowledgment:

The authors express their gratitude to the University of Cairo (Office of Vice President for Graduate Studies and Research) for providing partial financial support through "The Young Researchers' Program."

References

[1] Martindale: the Extra Pharmacopoeia, A. Wade (Ed.), 27th ed.; *The Pharmaceutical Press*, London, 1979.

[2] C. J. Nikles, M. Yelland, C. D. Marc, D. Wilkinson, *Am. J. Therap.*, 2005, **12**, 80-91.

[3] K. Brandt, *Drugs*, 2003, **63**, 23–41.

[4] A. A. Taylor, Baylor College of Medicine-Abstract from Munich Meeting (Thirteenth IUPHAR Congress of Pharmacology), 1998.

[5] National Institute of Health; National Heart, Lung and Blood Institute; National Asthma Initiative; Fact sheet 12-5075: "Asthma Care Quick Reference: Diagnosing and Managing Asthma," 2009.

[6] D. W. Cramer, B. L. Harlow, L.T. Ernstoff, K. Bohlke, W. R. Welch, E. R. Greenberg, *Lancet*., 1998, **351**, 104-107.

[7] M. Knochen, J. Giglio, F. R. Boaventure, *J. Pharmaceut. Biomed. Anal*., 2003, **33**, 191-197.

[8] V. Rodenas, M. S. Garcia, C. Sanchez-Pedreno, M. I. Albero, *Talanta*, 2000, **52**, 517-523.

[9] X. Huang, Y. Li, Y. Chen, L. Wang, *Sens. Actuators B,* 2008, **134**, 780-786.

[10] M. Ebadi, S. Sharma, S. Shavali, H. E. L. Refaey, *J. Neurosci. Res.,* 2008, **67**, 285-289.

[11] C. Bruhlmann, F. Ooms, P. A. Carrupt, B. Testa, M. Catto, F. Leonetti, C. Altomare, A. Carotti, *J. Med. Chem.*, 2001, **44**, 3195-3198.

[12] A. J. Shah, F. Crespib, C. Heidbrederb, *J. Chromatogr., B: Anal. Technol. Biomed. Life Sci.*, 2002, **781**, 151-163.

[13] S. K. Lunsford, H. Choi, J. Stinson, A. Yeary and D. D. Dionysiou, *Talanta*, 2007, **73**, 172-177.

[14] W. Sun, Z. Zhai, D.D. Wang, S.F. Liu, K. Jiao, *Bioelectrochemistry*, 2009, **74**, 295-300.

[15] M. Opallo, A. Lesniewski, *J. Electroanal. Chem.*, 2011, **656**, 2-16.

[16] A. A. Ensafi, B. Rezaei, H. Krimi-Maleh, *Ionics*, 2011, **17**, 659-668.

[17] X. Liu, Z. Ding, Y. He, Z. Xue, X. Zhao, X. Lu, *Colloids Surf. B*, 2010, **79**, 27-32.

[18] B. N. Chandrashekar, B. E. Kumara Swamy, N. B. Ashoka, M. Pandurangachar, *J. Mol. Liq.*, 2012, **165**, 168-172.

[19] C. Díaza, C. García, P. Iturriaga-Vásquez, M. J. Aguirre, J. P. Muena, R. Contreras, R. Ormazábal-Toledo, M. Isaacs, *Electrochim. Acta*, 2013, **111**, 846-854.

[20] P. Sun, D. W. Armstrong, *Anal. Chim. Acta*, 2010, **661**, 1-16.

[21] S. Pandey, *Anal. Chim. Acta*, 2006, **556**, 38-45.

[22] W. Qin, S. F. Y. Li, *Electrophoresis*, 2002, **23**, 4110-4116.

[23] D. Silvester, *Analyst*, 2011, **136**, 4871-4882.

[24] W. Sun, Y. Wang, S. Gong, Y. Cheng, F. Shi, Z. Sun, *Electrochim. Acta*, 2013, **109**, 298-304.

[25] L-. Ning Qu, J. Wu, X-. Ying Sun, M-. Ying Xi, W. Sun, *J. Chin. Chem. Soc*., 2010, **57**, 701-707.

[26] H. Beitollah, M. Goodarzian, M. A. Khalilzadeh, H. Karimi-Maleh, M. Hassanzadeh, M. Tajbakhsh, *J. Mol. Liq.*, 2012, **173**, 137-143.

[27] B. Kavosi, A. Salimi, R. Hallaj, K. Amani, *Biosens. Bioelectron*., 2014, **52**, 20-28.

[28] A. A. Ensafi , H. Bahrami, B. Rezaei, H. Karimi-Maleh, *Mater. Sci. Eng., C*, 2013, **33**, 831-835.

[29] W. Sun, Q. Jiang, M. Yang, and K. Jiao, *Bull. Korean Chem. Soc.*, 2008, **29**, 915-920.

[30] L. Liu, C. Duan, Z. Gaoi, *J. Serb. Chem. Soc.* 2012, **77**, 483-496.

[31] H. Liu, P. He, Z. Li, C. Sun, L. J. Shi, Y. Liu, G. Y. Zhu, J. H. Li, *Electrochem. Commun.* 2005, **7**, 1357-1363.

[32] W. Sun, M. X. Yang, R. F. Gao, K. Jiao, *Electroanalysis*, 2007, **19**, 1597-1602.

[33] W. Sun, Y. Li, Y. Duan, K. Jiao, *Biosens. Bioelectron.*, 2008, **24**, 988-993.

[34] F. Xiao, F. Zhao, J. Li, L. Liu, B. Zeng, Electrochim. Acta, 2008, **53**, 7781-7788.

[35] M. Arvand, M. Ghasempour Shiraz, *Electroanalysis*, 2012, **24**, 683-690.

[36] M. Musameh, J. Wang, *Anal. Chim. Acta*, 2008, **606**, 45-49.

[37] Q. Zhang, C. Shan, X. Wang, L. Chen, L. Niu, B. Chen, *Liq. Cryst.*, 2008, **35**, 765-772.

[38] Q. Zhang, C. Shan, X. Wang, L. Chen, L. Niu, B. Chen, *Liq. Cryst.*, 2008, **35**, 1299-1305.

[39] S. Kumar, S. K. Pal, *Tetrahedron Lett.*, 2005, **46**, 2607-2610.

[40] J. Motoyanagi, T. Fukushima, T. Aida, *Chem. Commun.*, 2005, 101-103.

[41] M. Elysi, M. A. Khalilzadeh, *Food Chemistry*, 2013, **141**, 4311-4317.

[42] E. Afsharmanesh, H. Karimi-Maleh, A. Pahlavan, J. Vahedi, *J. Mol. Liq.*, 2013, **181**, 8-13.

[43] H. J. Jeon, S. C. Yi, S.G. Oh, *Biomaterials*, 2003, **24**, 4921-4928.

[44] A. A. Ensafi, E. Khoddami, B. Rezaei, H. Karimi-Maleh, *Colloid. Surf*., B, 2010, **81**, 42-49.

[45] H. Beitollahi, H. Karimi-Maleh, H. Khabazzadeh, *Anal. Chem.* 2008, **80**, 9848-9851.

[46] M. Roodbari Shahmiri, A. Bahari, H. Karimi-Maleh, R. Hosseinzadeh, N. Mirnia, *Sens. Actuators, B: Chemical*, 2013, **177**, 70-77.

[47] R. Moradi, S. A. Sebt, H. Karimi-Maleh, R. Sadeghi, F. Karimi, A. Baharie, H. Arabi, *Phys. Chem. Chem. Phys.*, 2013, **15**, 5888-5897.

[48] M. Bijad, H. Karimi-Maleh, M. A. Khalilzadeh, *Food Anal. Methods*, 2013, **6**, 1639-1647.

[49] A. Salimi, E. Sharifi, A. Noorbakhash, S. Soltanian, *Biosens. Bioelectron.*, 2007, **22**, 3146-3153.

[50] T. You, O. Niwa, Z. Chen, K. Hayashi, M. Tomita, S. Hirono, *Anal. Chem* 75(2003) 5191.

[51] W. Xing, F. Li, Z. Yan, G. Q. Lu, *J. Power Sources*, 2004, **134**, 324-330.

[52] H. Kamal, E.K. Elmaghraby, S. A. Ali, K. Abdel-Hady, *Thin Solid Films* 2005, **483**, 330-339.

[53] A. Salimi, M. Roushani, S. Soltanian, R. Hallaj, *Anal. Chem*., 2007, **79**, 7431-7437.

[54] A. Salimi, M. Roushani, *Electroanalysis*, 2006, **18**, 2129-2136.

[55] A. Salimi, M. Roushani, R. Hallaj, *Electrochim. Acta*, 2006, **51**, 1952-1960.

[56] R. Vittal, H. Gomathi, K. J. Kim, *Adv. Colloid Interface*. *Sci*., 2006, **119**, 55-68.

[57] M. Plavsic, D. Krznaric, B. Cosovic, *Electroanal*ysis, 1994, **6**, 469-474.

[58] P. Manisankar, G. Selvanathan, C. Vedhi, *Talanta*, 2006, **68**, 686-692.

[59] N. F. Atta, A. Galal, R. A. Ahmed, *Bioelectrochemistry*, 2011, **80**, 132-141.

[60] N. F. Atta, A. Galal, R. A. Ahmed, *J. Electrochem. Soc.*, 2011, **158**, F52-F60.

[61] N. F. Atta, S. A. Darwish, S. E. Khalil, A. Galal, *Talanta*, 2007, **72**, 1438-1445.

[62] C. Li, Y. Ya , G. Zhan, *Colloids Surf., B: Biointerfaces* , 2010, **76**, 340-345.

[63] S. S. Hu, Y. Q. Yan, Z. F. Zhao, *Anal. Chim. Acta*, 1991, **248**, 103-108.

[64] H. C. Yi, K. B. Wu, S. S. Hu, D. F. Cui, *Talanta*, 2001, **55**, 1205-1210.

[65] S. H. Zhang, K. B. Wu, S. S. Hu, *Talanta*, 2002, **58**, 747-754.

[66] S. S. Hu, K. B. Wu, H. C. Yi, D. F. Cui, *Anal. Chim. Acta*, 2002, **464**, 209-216.

[67] D. Wei, A. Ivaska, *Anal. Chim. Acta*, 2002, **607**, 126-135.

[68] K. V. Axenov, S. Laschat, *Materials*, 2011, **4**, 206-259

[69] F. Li, J. Song, C. Shana, D. Gaoa, X. Xua, L. Niua, *Biosens. Bioelectron.*, 2010, **25**, 1408-1413.

[70] F. Marken, R. D. Webster, S. D. Bull, S. G. Davies, *J. Electroanal. Chem*., 1997, **437**, 209-218.

[71] R. Ojani, J. B. Raoof, Sh. Fathi, *J. Solid State Electrochem.*, 2009, **13**, 927-943.

[72] N. Yang, Q. Wan, J. Yu, *Sens. Actuators, B: Chemical*, 2005, **110**, 246-251.

[73] W. Qijin, Y. Nianjun, Z. Haili, Z. Xinpin, X. Bin, *Talanta*, 2001, **55**, 459-467.

[74] B. Saraswathyamma, I. Grzybowska, C. Orlewska, J. Radecki, W. Dehaen, K. G. Kumar, H. Radecka, *Electroanalysis*, 2008, **20**, 2317-2323.

[75] X. ShangGuang, H. Zhang, *Anal. Bioanal. Chem.*, 2008, **391**, 1049-1055.

[76] R. N. Goyal, V. K. gupta, M. Oyama, N. Bachheti, *Electrochem. Commun*., 2005, **7**, 803-807.

[77] R. N. Goyal, S. P. Singh, *Electrochim. Acta*, 2006, **51**, 3008-3012.

[78] B. C. Lourencao, R. A. Medeiros, R. C. Rocha-Filho, L. H. Mazo, O. Fatibello-Filho, *Talanta*, 2009, **78**, 748-752.

[79] R. T. Kachoosangi, G. G. Wildgoose, R. G. Compton, *Anal. Chim. Acta*, 2008, **618**, 54-60.

[80] P. Fanjul-Bolado, P. J. Lamas-Ardisana, D. Hernandez-Santos, A. Costa-García, *Anal. Chim. Acta*, 2009, **638**, 133-138.

[81] WHO Technical Report Series, No. 937; World Health Organization. Annex 4: "Supplementary guidelines on good manufacturing practices: validation; Appendix 4: Analytical method validation, 2006, 136-140.

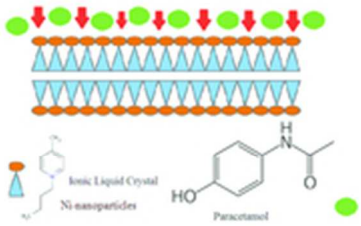

Ionic liquid crystals mimic the natural bio-based ionic liquid crystals such as cell membranes structures in their interactions with drugs.

18x13mm (300 x 300 DPI)